Analytica Chimica Acta 687 (2011) 168–176

Contents lists available at ScienceDirect

Analytica Chimica Acta

journal homepage: www.elsevier.com/locate/aca

Performance evaluation of fast Fourier-transform continuous cyclic-voltammetry pesticide biosensor

Bahman Ebrahimi[a], Seyed Abbas Shojaosadati[a,*], Parandis Daneshgar[b], Parviz Norouzi[c], Seyyed Mohammad Mousavi[a]

[a] Biotechnology Group, Chemical Engineering Department, Faculty of Engineering, Tarbiat Modares University, Tehran, Iran
[b] Institute of Biochemistry and Biophysic, University of Tehran, Tehran, Iran
[c] Center of Excellence in Electrochemistry, Faculty of Chemistry, University of Tehran, Tehran, Iran

ARTICLE INFO

Article history:
Received 5 October 2010
Received in revised form
30 November 2010
Accepted 4 December 2010
Available online 11 December 2010

Keywords:
Continuous cyclic voltammetry
Fast Fourier transform
Flow-through system
Acetylcholinesterase
Multiwall carbon nanotube
Optimization

ABSTRACT

In this work, a method for the fast monitoring of OPs in flow-injection systems was evaluated. The fast Fourier transform continuous cyclic-voltammetry (FFTCCV) at the carbon-paste electrode in a flowing solution system was used for determination of OPs. In this method the S/N ratio is enhanced by using of fast Fourier transform of the analyte and signal integration. FFTCCV can be considered as a new sensitive, accurate and fast method for determination of drugs and some pesticides. However, in order to obtain better sensitivity for a specific target, experimental parameters should be optimized. Response surface methodology (RSM) was applied to optimize three effective parameters (enzyme activity, multiwall carbon nanotube quantity and acidic sol–gel quantity). The optimum values for the tested parameters were enzyme amount H0.169 U cm^{-2}, multiwall carbon nanotube (MWCNT) 0.607 mL and acidic sol–gel 1.012 mL. The optimum feed pH, feed flow rate, ATChCl concentration and sweeping-rate were found to be 7.4, 0.34 mL min^{-1}, 0.750 mM and 10 V s^{-1}, respectively. The long-term stability of this flow-through system was 80% of its initial response after 120 days. Based on an incubation time of 12 min, it was found that the detection limit for paraoxon was equal to 1.7×10^{-7} mg L^{-1} (6.2×10^{-13} M). The developed biosensor exhibited good repeatability and reproducibility. This study provides a new, modern, sensitive tool for the analysis of organophosphate pesticides.

1. Introduction

The great success of organophosphorous (OP) compounds in agricultural applications has led to an increase in the production and spread of these insecticides. OP compounds exhibit acute toxicity and can irreversibly inhibit acetylcholinesterase (AChE), which is essential for the functioning of the central nervous system, often causing respiratory paralysis and death. Common analytical techniques for the determination of OP compounds such as gas and liquid chromatography [1] are sensitive and reliable; however, these methods are time-consuming and require expensive equipment, highly trained personnel, and complicated sample pretreatments and are not suitable for field conditions. Based on the inhibition of enzymatic activity by OP, paraoxon was monitored by measuring the oxidation current of thiocholine. Aldridge [2] has described the inhibition mechanism:

$$\text{Acetylthiocholine chloride} + H_2O \xrightarrow{\text{AChE}} \text{thiocholine (red)} + \text{acetic acid} + Cl^- \quad (1)$$

$$2\,\text{Thiocholine (red)} \rightarrow 2\,\text{thiocholine (ox)} + 2e^- + 2H^+ \quad (2)$$

$$E + (OP)X \rightarrow E(OP) + X \quad (3)$$

where E is the enzyme, (OP)X is organophosphate or carbamate, and X is the leaving group.

At present, detection and evaluation of OP exposure is generally performed at dedicated centralized laboratories using large, automated analyzers such as liquid or gas chromatography coupled with mass spectrometry (HPLC/GC/MS), requiring sample transportation and processing which ultimately increases the waiting time for results. Rapid near-patient or field biomonitoring tools for the first responders are highly desirable to facilitate rapid screening to initiate appropriate treatments. Currently, three approaches have been developed for biomonitoring of OP exposure: (1) assay of enzyme activity, (2) measure-

* Corresponding author. Tel.: +98 21 82883341; fax: +98 21 82883381.
E-mail address: shoja_sa@modares.ac.ir (S.A. Shojaosadati).

0003-2670/$ – see front matter © 2010 Elsevier B.V. All rights reserved.
doi:10.1016/j.aca.2010.12.005

ment of metabolites and (3) detection of phosphorylated adducts [3].

Despite their clear advantages, the development of a successful biosensor has encountered several problems, such as low response stability (due to biomolecule leaking or deactivation), low mechanical stability, high diffusion resistance of the substrate/biocomponent assembly, interfering signals arising from other compounds present in real samples and, especially for cholinesterase-based biosensors, multi-stage procedures. Thus, the biosensor design is a key factor to overcome these drawbacks.

Flow methods improve the sensitivity and reproducibility of the method as a consequence of the highly controllable conditions of mass transport provided by the flowing solutions [4]. The combination of biosensors with flow-injection analysis (FIA) techniques offers the possibility to control the whole procedure, simplifying the sequence of steps and allowing an easier optimization of the reaction conditions [5].

Recently, Du et al. have developed a CNT-based amperometric sensor combined with a microflow-injection device and double test mode via regeneration of AChE from OP-inhibited saliva samples and demonstrated its low-cost, simplicity, and sensitivity for assessment of subclinical OP exposure [3]. Compared with routine approaches for evaluating the decrease from an average or control value, this new technology based on double-test mode excludes inter or intraindividual variation in the normal levels of ChE. Wang et al. reported the development of a CNT-based amperometric sensor with a flow injection system for characterization of enzyme activities in rat saliva samples. This flow-injection system provided great advantages for onsite, real-time, and continuous detection of biomolecules and required only a small volume of the sample. This sensor took advantage of the electrocatalytic properties of CNTs, which made it feasible for a sensitive electrochemical detection of the products from enzymatic reactions at low potential [6]. Also, Shitanda et al. [7] presented a preliminary report on a screen-printed algal biosensor. An algal ink was prepared and immobilized on a carbon electrode by screen-printing. The photosynthetic oxygen evolution of the algal cell could be monitored on a flow injection analysis system [7]. Recent studies have demonstrated that CNTs can improve the direct electron transfer reaction of some biomolecules on an electrode surface; this is attributed to their unique electronic structure, high electrical conductivity, and redox-active sites.

Hence there is a need for a continuous, user friendly, sensitive screening method which is capable of performing rapid analyses to detect pollution events. This initial screening will reduce the time wasted in analyzing hundreds of pesticide-free samples by conventional methods. This goal is becoming more attainable as screening methods are being developed based on fluorescence, immunoenzymatic and chemiluminescence flow injection techniques [8]. There is a growing interest in the use of packing as a support material to enhance reaction rates. Packing provides a better distribution of the catalyst, particularly when the reaction is performed in column or fixed bed reactors [9]. For industrial applications, it is important to design an efficient enzymatic immobilization system and to obtain the optimum immobilization and process conditions for better response. Improvements in the immobilization and process parameters would enhance the efficiency of the process in flow-through systems.

Because of the selective detector, voltammetric techniques are useful for the samples. Owing to the movement of the analyte zone in an electrochemical flow cell for flowing solutions, the application of these techniques requires fast analyte accumulation and fast potential sweeping (which is not appropriate for large electrodes) [10–13]. Stripping voltammetric techniques have the advantages of being both rapid and economical in the determination of most organic and inorganic compounds in aqueous systems, with sensitivity for trace amounts. In fact, because of the passage of an analyte through the zone in front of the electrode in an electrochemical flow cell, the application of such techniques in flowing solutions requires fast accumulation of the analyte and fast potential sweeping, which is not appropriate in traditional voltammetry but is applicable in fast Fourier-transform (FFT) voltammetry [14]. Application of a Fourier-transform potential-sweeping waveform in a flowing solution in cyclic or square-wave voltammetric mode can be of great help [12]. Electrochemical conditioning (EC) permits the maintenance of a clean and active electrode surface for long periods of time. The background current in voltammetric measurements can provide useful information about the adsorption processes and changes occurring in the double layer at the electrode surface. In square-wave voltammetric measurement, for instance, the change occurring in the double-layer capacitance has been used for the determination. In addition, a low adsorption of species existing in the solution and on the electrode surface can strongly affect the cathodic and anodic currents of the redox reaction that occurs [11–13]. Recently, a number of electrochemical methods, such as electrochemical impedance spectroscopy, mathematical modeling of the AC voltammetry, and modulated linear-ramp voltammetry, have been combined with FFT methods for increasing the sensitivity and simplicity of data analysis [15].

This research describes a new electrochemical method, based on FIA and FFT Cyclic voltammetry, for the determination of paraoxon. In this work, the combination of the fast Fourier transform continuous cyclic-voltammetry (FFTCCV) and a fixed-bed reactor in a flow-through system greatly catalyzed the reaction of the enzymatically generated thiocholine product, thus increasing the detection sensitivity. In this method the S/N ratio is enhanced by using of fast Fourier transform of the analyte and signal integration. For this work, we used the highly developed version of an old electrochemical system (the computer program is more advanced in the algorithm for integration and filtering). As a consequence, the noise level was less; resulting in a better S/N. Fortunately it was feasible to determine paraoxon at a detection limit lower than those of other reported methods. FFTCCV can be considered as a new sensitive, accurate and fast method for determination of drugs and some pesticides. However, in order to obtain better sensitivity for a specific target, experimental parameters should be optimized. Therefore in this study, the main objectives were to better understand the immobilized and process variable effect and relations with response. All the results obtained in this study would provide a sound basis for further exploration.

2. Materials and methods

2.1. Materials

Multiwall carbon nanotubes at 95% purity, with a length of 1–10 μm, an external diameter of 37 nm, and wall Nos. 3–15, were obtained from Plasma Chem. GmbH Company, Germany. Tetraethylorthosilicate (TEOS) at 99% purity was supplied from Merck Company, Germany. Triton X-100 was obtained from Aldrich Chemicals Co. Acetylthiocholine chloride (ATChCl) at 99% purity was purchased from Fluka, UK. Dimethylformamide (DMF) was obtained from Sigma, USA. Acetylcholinesterase (type V-S: electric eel source, 425 U mg^{-1} solid), was purchased from Sigma–Aldrich, Inc., USA. Ceramic cylinders with an average length of 1.8 mm, an external diameter of 1.9 mm, and an internal diameter of 1 mm were obtained from Tailor China Shop, Iran. Phosphate buffers with various pH values were prepared according to the manual.

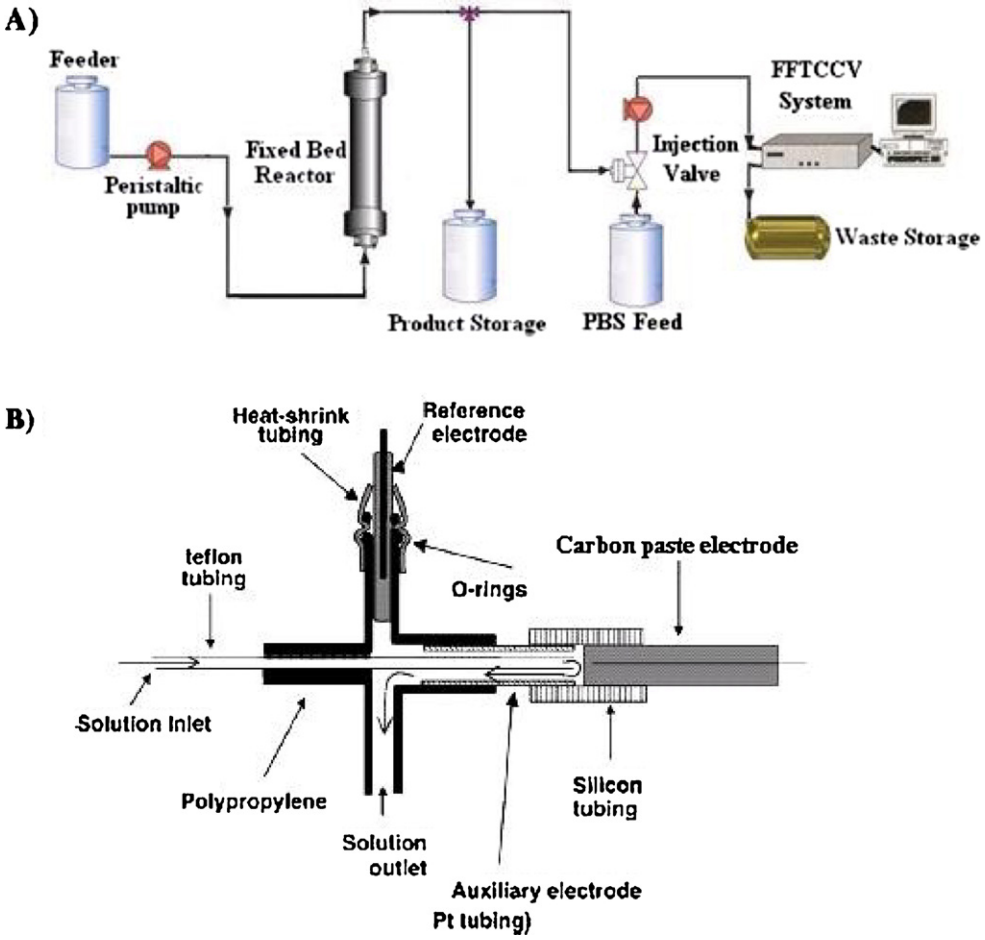

Fig. 1. Schematic diagram of (A) flow-through system; (B) the electrochemical cell.

2.2. Procedures

2.2.1. Preparation of MWCNT–silicate sol and enzyme doped thin sol–gel film

MWCNTs were sonicated in a water bath for 20 min and in ethanol for another 30 min and dried at 80 °C for 30 min. The MWCNT suspension was prepared by adding 3 mg of dried MWCNTs to a DMF solution (2 mg MWCNT/1 mL DMF solution) [16] and then cooling to 4 °C. A homogenous TEOS silica sol was prepared by mixing 2 mL of TEOS, 1 mL of H_2O, 50 μL of 0.1 M HCl, and 25 μL of 10% Triton X-100 (final concentration 0.08%). Mutual solvent ethanol was not used in our experiments. In this solventless hydrosol procedure, TEOS is added to distilled water and stirred magnetically to form a gray, two-phase dispersion at room temperature. When the solution is acidified, the dispersion is transformed into a clear solution within 30 min. This mixture is stirred for 1 h until a clear sol is formed. The sol can be stored for several months at −20 °C. An aliquot of 1012 μL of stock sol–gel solution was vortexed with 40 μL of enzyme stock solution (0.169 U cm^{-2}) and 200 μL of 0.1 M phosphate buffer solution (pH 7.4) containing 5 μL glycerol, and 0.607 mL of MWCNT suspension was mixed with the silicate sol solution to prepare the silicate-MWCNT sol. The mixture was spread on to 5.3 g of packing surface. This film was allowed to polymerize at 4 °C for 1–2 h. Then the packing was transferred onto a clean surface and allowed to dry for 24 h at 4 °C in a refrigerator. Finally the packing was immersed in PBS (pH 7.4) and kept at 4 °C in a refrigerator in order to remove the excess materials from the immobilized surface [17].

2.2.2. Preparation of the enzymatic reactor and flow-through system

In the flow system (Fig. 1A), a peristaltic pump was used to impel solutions. The various system elements were connected by silicon tubes. The fixed-bed reactor was constructed using a serum tube of 4.79 cm length, with external and internal diameters of 1.41 and 1.19 cm, respectively. All of the coated ceramic packing was carefully packed into the reactor. Then the fixed-bed reactor was connected to the flow line after the peristaltic pump, as shown in Fig. 1A. Reactor feed was prepared by dissolving 0.0079 g of ATChCl in 40 mL of phosphate buffer (0.1 M and pH 7.4). The reactor exit was connected to an injection valve as shown in Fig. 1A.

2.2.3. Flow injection setup

For the preparation of the carbon-paste electrode, a sampler head tube (5 cm in length) with a hole at one end (2 mm in diameter) was filled with carbon paste to serve as the electrode body. Electrical contact was provided by a copper piston within the center of the tube. Carbon paste was prepared by adding 0.05 g of mineral oil to 0.15 g graphite powder. The mixture was homogenized carefully and packed into the hole of the electrode holder. The electrode surface was smoothed with a weighing paper. The electrode was washed with water before being placed in the cell. Additionally, an Ag(s)|AgCl(s)|KCl (aq., 1 M) reference electrode was used in all measurements, while the auxiliary electrode was made of a Pt wire (1 cm in length and 0.5 mm in diameter). In Fig. 1B, the electrochemical cell of the flow-injection analysis setup is presented. For this analysis, a 10-roller peristaltic pump (UltrateckLabs Co., Iran)

and a six-way injection valve (Supelco Rheodyne Model 5020) with a 50-μL sample injection loop were used. The flow rate of the eluent solution during the experiments was set to 3.4 mL min^{-1}, and the cell volume was 100 μL. Phosphate buffer (0.1 M, pH 7.4) was pumped into the system as feed.

2.2.4. Data acquisition and processing

For the data acquisition, a setup of a PC Pentium IV 900 MHz microcomputer, equipped with a data-acquisition board (PCL-818HG, Advantech. Co.) and a custom-made potentiostat was used. All data-acquisition and data-processing programs were developed in the Delphi 6® programming environment [18]. Three parts are evident in the potential waveform: (a) potential steps, Ec_1 and Ec_2 (which are used for the oxidation and reduction of the electrode surface, respectively), during which the electrochemical cleaning of the electrode surface takes place; (b) Es, where the analyte accumulation takes place; and (c) the potential ramp, where the current measurements occur. The electrode conditioning starts with the cleaning process, in which the electrode potential is held at a positive potential, Ec_1 (1600 mV), at least for 100 ms. Then, for the reduction and desorption of any fouling component on the surface, it is held at the Ec_2 potential (−400 mV) for 100 ms. Finally, the current measurements are performed during potential ramp. The starting point for the electrochemical oxidation process of the carbon-paste electrode surface is as given in Eq. (2).

In this method, the signal calculation is measured by the integration of the net current changes over the scanned potential range. It must be noted that, in this case, the current changes (as a result of the injected analyte) in the voltammogram can be caused by oxidation and reduction processes, which happen on the electrode surface. Indeed, the influence of the adsorbed analyte on the oxidation and reduction peaks of the component can be eliminated by using a cleaning step in the applied potential. Furthermore, the scan rate is proportional to the kinetics of electron transfer and the detection of a given concentration of analyte in the zone passing through the electrode [19,20].

2.2.5. Inhibition measurements

The degree of irreversible inhibition, I (%), of the OP insecticide on the enzymatic activity of immobilized AChE was measured as a relative decrease of the response after a contact of the biosensor with paraoxon. The initial response, I_0, of 1 mM ATChCl (at a flow rate of 0.4 mL min^{-1}) was first measured. After the system was washed with carrier buffer at 0.4 mL min^{-1} for 10 min, 0.1 mL of paraoxon solution was injected and stopped in the packed bed reactor for 12 min (the optimum incubation time) followed by washing with the carrier buffer at 0.4 mL min^{-1} for 15 min; again, the response of 1 mM ATChCl was measured (I_f). The inhibition was calculated by Eq. (4):

$$I(\%) = 100 \times \frac{(I_0 - I_f)}{I_0} \quad (4)$$

3. Results and discussion

3.1. Electrochemical behavior of the system

Fig. 2A depicts a CV sequence recorded during the flow analysis for the thiocholine determination. The injection volume was 50 μL of reactor exit solution into the eluent solution. In the plot, the time axis represents the time of the flow-injection experiment. When thiocholine was not present, the shape of the CV curves was typical for a carbon-paste electrode in PBS media.

Fig. 2B illustrates the absolute current changes in the CV curves after the subtraction of the average background of the four CVs (in the absence of the analyte). The four first CVs was saved and

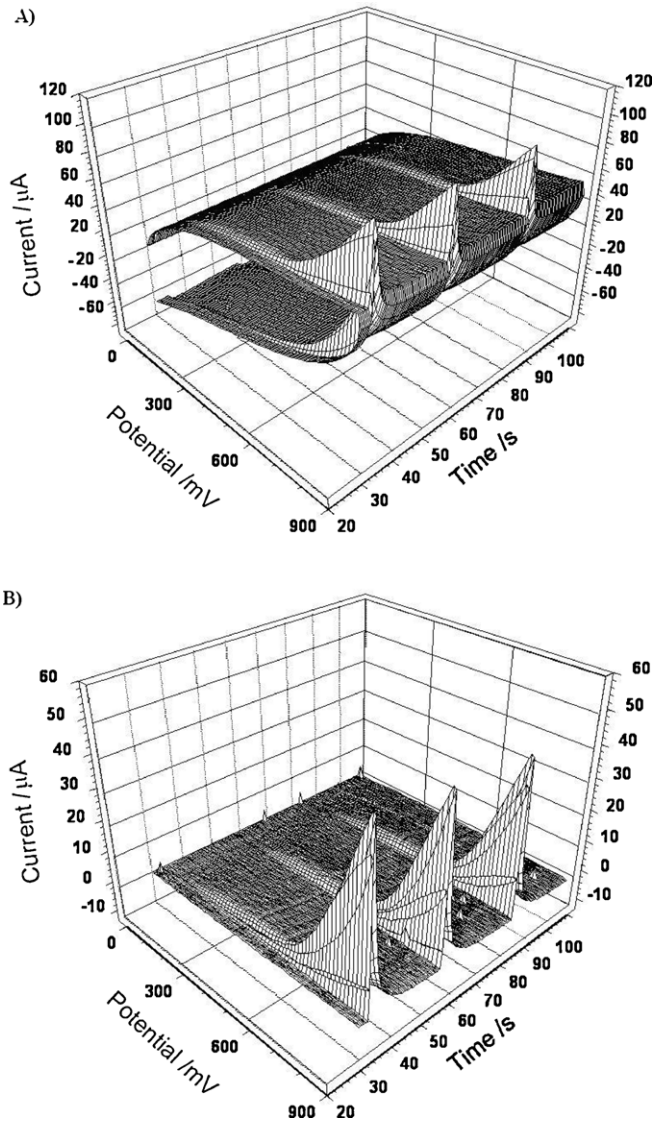

Fig. 2. (A) Cyclic voltammogram with a carbon-paste electrode, recorded during a flow-injection experiment. Each scan was preceded by a conditioning of 100 ms (at 1600 mV) followed by 100 ms (at −400 mV). These CVs were recorded at the optimum conditions and flow rate. (B) Curves resulting from the subtraction of averaged CV (in the absence of the analyte) from the CV test in (A).

the current or charge will be saved in software of program then by recording the other votammograms the current will compare by the first saved voltammogramms and the current or charge will subtracted from the first ones. If any distinguish change (by injection the component and adsorption or redox of the component on the) will be appear the difference between these two will be more than the recorded voltammograms of background. These data acquisition is possible in FFT system which helps to improve the signal to noise ratio. This improved way of presenting the electrode response provides more details about the change of current by the injections and redox product, thiocholine. The curves show that the current changes mainly took place in the potential regions of the oxidation and reduction of thiocholine. The oxide-formation process became severely inhibited when the electrode–solution interface was exposed to thiocholine, showing an irreversible redox peak on the surface of the electrode. In detail, the inhibition effect of AChE caused a significant change in the current with the generation of electroactive component thiocholine at the potential region, and, as a consequence, profound changes in the shape of the CVs

Table 1
The level of control variables.

High axial (+α)	High factorial (+1)	Center (0)	Low factorial (−1)	Low axial (−α)	Variable
0.3430	0.2752	0.1736	0.0720	0.0029	E (U cm^{-2})
1220	1050	800	550	380	CNT (μL)
3446	2800	1850	900	254	S (μL)

took place. In chromatographic analysis, where a mixture of compounds is present in the sample, the universality of the detector is beneficial. In general, the thermodynamic and kinetic parameters of adsorption, the mass-transport rate, and the electrochemical behavior of the adsorbed species influence the analyte response. The free energy and the adsorption rate depend on the electrode potential, the electrode material and, to some extent, on the choice of the concentration and type of the supporting electrolyte.

3.2. Optimization of immobilization

3.2.1. Experimental design

Central composite, Box–Behnken and Doehlert designs are among the principal RSMs used in the experimental design. The most popular response surface method is the central composite design. This design consists of the following parts: (1) a full factorial or fractional factorial design, (2) an additional design (often a star design) in which the experimental points are at a distance α from its center, and (3) a central point. The α values are 1.41, 1.68, and 2.00 for two, three and four variables, respectively.

A 5-level ($-\alpha$, −1, 0, +1, +α) design was employed in this study, requiring 20 experiments. For statistical calculations, the relation between the coded values and actual values are described by the following equation:

$$x_i = \frac{X_i - X_{i0}}{\Delta X}, \quad (5)$$

where x_i is a coded value of the variable, X_i is the actual value of the variable, X_{i0} is the actual value of X_i at the center point, and ΔX is the step change of the variable. The variables and the levels that were selected for use in the AChE immobilization study are shown in Table 1.

The design matrix is shown in Table 2. The quadratic equation for the variables is as follows:

$$Y = \beta_0 + \Sigma\beta_i x_i + \Sigma\beta_{ii} x_i^2 + \Sigma\beta_{ij} x_i x_j \quad (6)$$

where Y, β_0, β_i, β_{ii}, and β_{ij} are the predicted response, a constant, a linear coefficient, a squared coefficient, and an interaction coefficient, respectively. Eq. (6) was used to build surfaces for variables. This model was likely to be useful as an approximation of the true response surface in a relatively small region, and it is widely used in RSM for the following reasons:

1. The second-order model is very flexible. It can take on a wide variety of functional forms, so it will often work well as an approximation of the true response surface.
2. It is easy to estimate the parameters (the β's) in the second-order model. The method of least squares can be used for this purpose.
3. There is considerable practical experience indicating that second-order models work well for solving real response surface problems.

We used the central composite design to find suitable variables. The results of the CCD experiments consisted of the coded, actual and experimental data. These were used to determine the effects of three variables (the amount of enzyme, MWCNT and the acidic sol–gel) on the response, and are presented in Table 2. The software Minitab (version 14) was used to analyze the results.

3.2.2. Optimization and model fitting

Response-time curves with constant ATCh concentration (1 mM) and different values of enzyme activity, multiwall carbon nanotube quantity and acidic sol–gel quantity were used in 30 min after process initiation.

The data were fitted with a second-order polynomial function (Eq. (7)).

$$Y = 0.45 + 0.072A - 0.122B - 0.009C + 0.002A^2 + 0.072B^2 - 0.072C^2 - 0.076AB - 0.078AC + 0.071BC \quad (7)$$

The analysis of variance (Table 3) indicated that the model terms of A, B, B^2, C^2, AB, AC and BC were significant ("probe > F" less than

Table 2
The coded values, actual values, and absorbance response of different values of the variables.

Absorbance response	Actual value of the sol–gel (μL)	Actual value of the MWCNT (μL)	Actual value of the enzyme (U cm^{-2})	Coded value of the sol–gel (μL)	Coded value of the MWCNT (μL)	Coded value of the enzyme (U cm^{-2})	Run no.
0.525	1850	1220	0.1736	0	1.68	0	1
0.960	900	550	0.2752	−1	−1	1	2
0.453	1850	800	0.1736	0	0	0	3
0.630	1850	800	0.3430	0	0	1.68	4
0.447	1850	800	0.1736	0	0	0	5
0.453	1850	800	0.1736	0	0	0	6
0.393	2800	1050	0.0720	1	1	−1	7
0.465	2800	550	0.0720	1	−1	−1	8
0.252	900	1050	0.0720	−1	1	−1	9
0.330	3446	800	0.1736	1.68	0	0	10
0.165	254	800	0.1736	−1.68	0	0	11
0.504	2800	550	0.2752	1	−1	1	12
0.447	1850	800	0.1736	0	0	0	13
0.786	1850	380	0.1736	0	−1.68	0	14
0.243	2800	1050	0.2752	1	1	1	15
0.495	900	550	0.0720	−1	−1	−1	16
0.456	1850	800	0.1736	0	0	0	17
0.450	1850	800	0.1736	0	0	0	18
0.288	1850	800	0.0029	0	0	−1.68	19
0.300	900	1050	0.2752	−1	1	1	20

Table 3
Estimated regression coefficients.

Term	Cons.	A	B	C	$A \times A$	$B \times B$	$C \times C$	$A \times B$	$A \times C$	$B \times C$
Coef.	0.45	0.072	−0.122	−0.009	0.002	0.072	−0.072	−0.076	−0.078	0.071
SE coef.	0.03354	0.02225	0.02225	0.02225	0.02166	0.02166	0.02166	0.02907	0.02907	0.02907
T	13.449	3.215	−5.511	−0.410	0.104	3.312	−3.347	−2.605	−2.683	2.451
P-value	0.000	0.009	0.000	0.691	0.919	0.008	0.007	0.026	0.023	0.034

0.05), but A^2 and C were not significant. Thus, the related terms were eliminated because they had P-values more than 0.1 and also caused a decrease in the adjusted R^2 of the model. Therefore, the simplified second-order polynomial equation for protease production (Y) in terms of actual factors was expressed as follows:

$$Y = 0.45 + 0.072A - 0.122B + 0.072B^2 - 0.072C^2 - 0.076AB - 0.078AC + 0.071BC \quad (8)$$

where A, B and C are enzyme amount, MWCNT and acidic sol–gel content, respectively.

It is always necessary to examine the fitted model to ensure that it provides an adequate approximation to the true system and verifies that none of the least squares regression assumptions is violated. The ANOVA results of the developed models that were calculated using a statistical software, Minitab 14, are shown in Table 4. It illustrates that all fitted models are significant in 95% confidence level.

R^2 is a measure of the amount of reduction in the variability of y obtained by the regressor variables x_1, x_2,..., x_k in the model. However, a large value of R^2 does not necessarily imply that the regression model is good one. Adding a variable to the model will always increase R^2, regardless of whether the additional variable is statistically significant or not. Thus it is possible for models that have large values of R^2 to yield poor predictions of new observations or estimates of the mean response. Because R^2 always increases when terms are added to the model, some regression model builders prefer to use an adjusted R^2. In general, the adjusted R^2 statistic will not always increase as variables are added to the model. In fact, if unnecessary terms are added, the value of adjusted R^2 will often decrease. When R^2 and adjusted R^2 differ dramatically, there is a good chance that non-significant terms have been included in the model. Such tests would be useful in determining the value of each of the regressor variables in the regression model. For example, the model might be more effective with the inclusion of additional variables, or perhaps with the deletion of one or more of the variables already in the model. Adding a variable to the regression model always causes the sum of squares for regression to increase and the error sum of squares to decrease. It must be decided whether the increase in the regression sum of squares is sufficient to warrant using the additional variable in the model. Furthermore, adding an unimportant variable to the model can actually increase the mean square error, thereby decreasing the usefulness of the model.

The regression equation obtained from analysis of variance (ANOVA) indicated that the multiple correlation coefficient of R^2 is 0.9281 i.e. the model can explain 92.81% variation in the response. It should be noted that a R^2 value greater than 0.75 indicates the aptness of the model. The adjusted R^2 and value is 0.8634. The high value of R^2 indicates that the quadratic equation is capable of representing the system under the given experimental domain.

The ANOVA results in Table 4 confirmed a satisfactory adjustment of the simplified quadratic model to the experimental data. It should be considered that the polynomial model is a reasonable approximation of the true functional relationship on a relatively small region of the entire space of the independent variables.

The optimum values of enzyme amount, MWCNT and sol–gel content determined by the Minitab 14 were 0.169 U cm^{-2}, 0.607 mL and 1.012 mL, respectively.

3.3. Immobilized surface morphology

The reactor-bed surface was characterized microscopically; Fig. 3 shows the SEM images of the packing surface structure increased the specific surface area of the catalyst and was instrumental in enhancing the reaction rate in the enzymatic reactor

3.4. pH and sweeping-rate effect

The bioactivity of the immobilized AChE depends on the solution pH. The optimal pH is usually in the range of 6.5–8. Thus, the effect of pH was examined in the range of pH 4–10.The results are shown in Fig. 4, which show that the optimal pH value was 7.4. Thus, pH 7.4 was selected for detection.

An acetylthiocholine concentration of 750 μM was used for the investigation of the sweeping-rate effect. The detector responses to the potential sweep rates were recorded at different sweep rates in the range of 4–20 V s^{-1}. The results showed that the detector exhibited the maximum sensitivity at the sweep-rate value of 10 V s^{-1}. The effects of the sweep rate on the detection performance can be considered from two aspects: first, speed in data acquisition, and second, kinetic factors of the thiocholine redox behavior. Also, the use of this detection method in conjunction with fast separation techniques such as capillary electrophoresis requires the employment of high sweep rates. From this point of view, it is important to check how the sensitivity of the method is affected by the sweep rate. Nonetheless, the potential sweep rate is the determining factor which defines the sensitivity of the detection system, basically because of the kinetic factors of redox reaction and the instrumental limitations.

Table 4
Analysis of variance (ANOVA) for response.

Source	DF	Seq. sum of square	Adj sum of square	F-value	P-value
Regression	9	0.578215	0.578215	9.50	0.001
Linear	3	0.276478	0.276478	13.63	0.001
Square	3	0.166548	0.166548	8.21	0.005
Interaction	3	0.135189	0.135189	6.66	0.009
Residual error	10	0.067627	0.067627		
Lack-of-fit	5	0.067561	0.067561	1023.65	0.000
Pure error	5	0.000066	0.000066		
Total	19	0.645842			

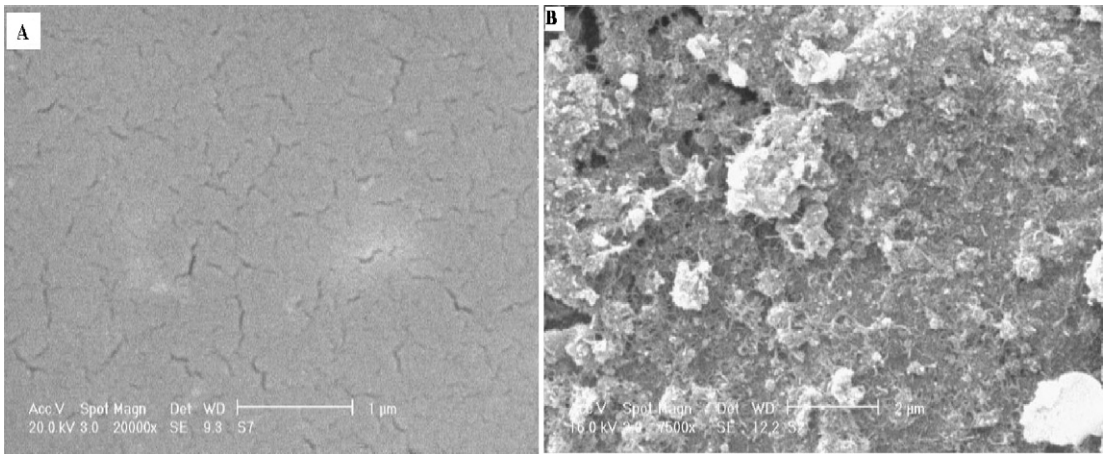

Fig. 3. SEM images of (A) ceramic surface, (B) enzyme encapsulated in MWCNT–sol–gel on ceramic surface.

3.5. Effect of the flow rate

The main factor that affects the analytical performance of the flow-through sensor system is the flow rate. This work examined the effect of flow rate on the current response in the range of 0.05–1.6 mL min^{-1}. As shown in Fig. 5, the feed-flow rate had an inverse effect on the current response. With a decrease in the feed-flow rate from 1.6 mL min^{-1} to 0.34 mL min^{-1}, the response increased and then leveled off. Therefore, an optimum value occurred at the flow rate of 0.34 mL min^{-1}. The difference in behavior of the system with respect to different feed-flow rates can be explained by the high flow rate has short retention time, making molecules insufficient time to diffuse and react.

3.6. Effect of the feed concentration

Fig. 6 presents the optimal conditions for the effect of ATChCl concentration on response. In the immobilized layer, the enzyme catalyzes the hydrolysis of ATChCl to thiocholine and acetic acid. Thus, ATChCl was used as a substrate for the characterization of the enzyme. With increasing concentration of ATChCl, the response increased linearly (R^2 = 0.9745) in the range of 7–750 μM and then reached a constant value. The linear slope (sensitivity) was 0.0325 microamperes change per micromole of ATChCl. The ATChI concentration of 750 μM was selected for the flow-through system for obtaining the maximum response. The difference in behavior of the biosensor towards different concentrations of substrate can be explained by the slower diffusion of the substrate to the acidic sol–gel layer, especially at low substrate concentrations and also possibly to slower reaction kinetics in the alkoxysilane-derived matrices when less substrate was available.

At a concentration of 750 μM ATChCl, the flow-through biosensor showed a response current of 24.5 μA and a quite good reproducibility. The flow-through biosensor prepared in the same batch demonstrated a standard deviation of 2.41% for the three successive assays.

3.7. Stability of the flow-through system

The stability of the flow-through system was verified by monitoring the current response at regular intervals of time over a period of 120 days. After the flow-through system was stored at 4 °C under dry conditions, its response was stable over a 7-day storage period and then decreased to 91% after 50 days. When the flow-through system was stored for 75 days, it retained 88% of its initial current response. The response decreased to 80% after four months, an enzyme stability that should be satisfactory for most applications. The enhanced stability of the proposed biosensors was mainly due

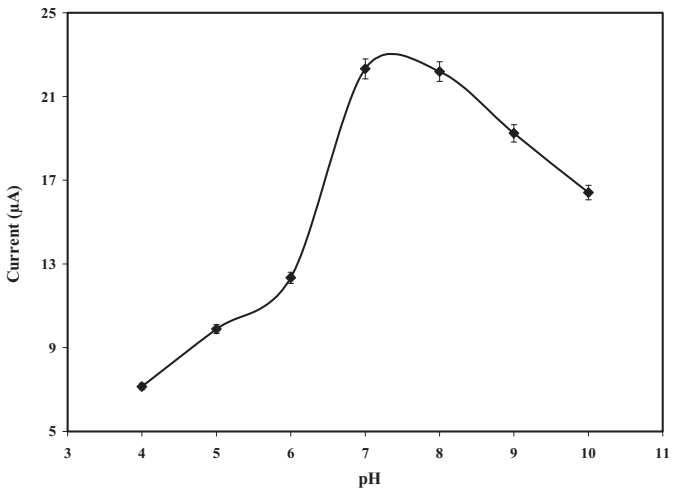

Fig. 4. Comparison of different reactor feed pH on current response of the flow-through system (feed-flow rate, 0.34 mL min^{-1}; immobilization condition, optimum; ATChCl concentration, 0.75 mM; residence time in reactor, 6 min).

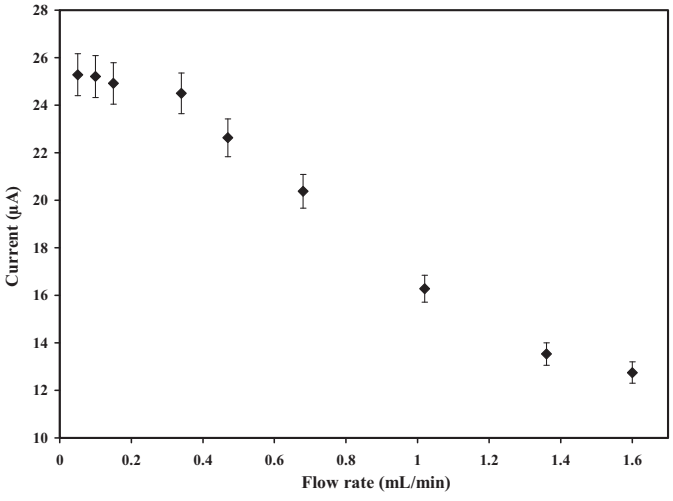

Fig. 5. Effect of flow rate on the current response of the flow-through system (ATChCl concentration, 0.75 mM; feed pH, 7.4; immobilization conditions, optimum; process-initiation time, constant).

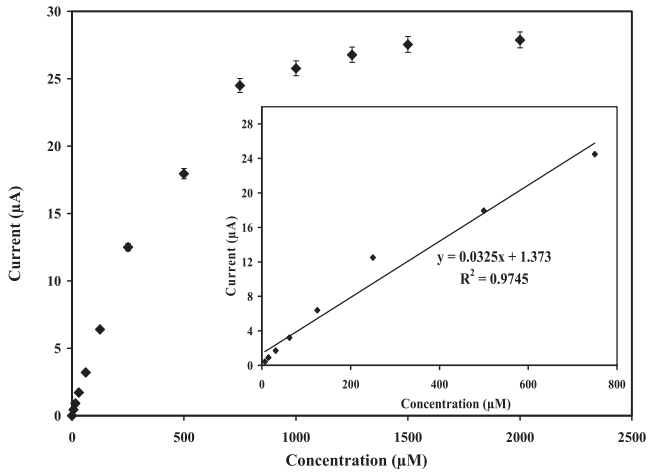

Fig. 6. Effect of the feed concentration on the current response of the flow-through system (feed-flow rate, 0.34 mL min^{-1}; immobilization conditions, optimum; feed pH, 7.4; residence time in reactor, 6 min; process-initiation time, constant).

to the biocompatible nature of the immobilized method and the nanoporosity of the immobilized surface.

3.8. Determination of paraoxon

3.8.1. Effect of inhibition time on response

One of the most influential parameters in pesticide analysis is inhibition time. With increased incubation time in the paraoxon solution the current response decreased greatly, and paraoxon displayed an increasing inhibition with increasing time. When the incubation time was longer than 12 min, the curve (not shown) trended towards a stable value, indicating that binding interactions with active target groups in the enzyme were reaching saturation. This tendency of the current response to decrease reflects a change in enzymatic activity. Therefore, the change observed in the system can be used as an indicator for quantitative measurement of paraoxon pesticide.

3.8.2. Inhibition curve

In order to demonstrate the usefulness of this system for the determination of paraoxon, the flow-through system biosensor was exposed to paraoxon concentrations (using the optimum conditions established in the above) of 2.5×10^{-7} to 20 mg L^{-1}. The inhibition response of the flow-through system biosensor towards paraoxon is shown in Fig. 7. Clearly, Fig. 7 showed linearity with −log [paraoxon] in the concentration range of 2.5×10^{-7} to 0.05 mg L^{-1}, with a detection limit of 1.7×10^{-7} mg L^{-1} (6.2×10^{-13} M), based on a 0.1 mL paraoxon injection of 6.2×10^{-17} mol (10% inhibition level of enzyme, 12 min incubation times). The linear equation was as follows: inhibition (%) = 12.386 log [paraoxon] + 93.836 (%), with a correlation coefficients of 0.9841 (Fig. 7).

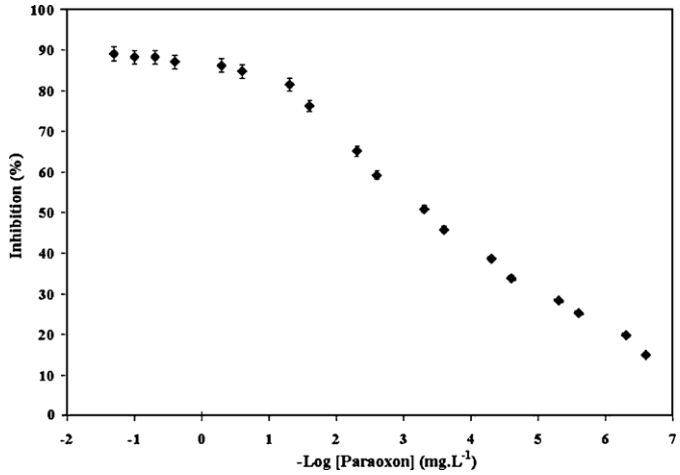

Fig. 7. Inhibition profile of the flow-through biosensor system with various concentrations of paraoxon (feed flow rate, 0.34 mL min^{-1}; immobilization conditions, optimum; ATChCl concentration, 0.75 mM; feed pH, 7.4; incubation time, 12 min).

4. Conclusions

A simple strategy for designing a highly sensitive electrochemical biosensor for organophosphate pesticides (OPs) based on acetylcholinesterase (AChE) immobilized onto a packing by a composite MWCNT silicate sol film was evaluated (Here, MWCNTs play a dual role in both enzyme immobilization and efficiency of the reaction. MWCNTs function as carriers for AChE immobilization to provide a suitable microenvironment to retain the AChE activity and, as porous surfaces in sol–gel film, lead to an increase in the efficiency of the reaction). The combination of FFTCCV and a fixed-bed reactor in a flow-through system greatly catalyzed the reaction of the enzymatically generated thiocholine product, thus increasing the detection sensitivity. In this method the S/N ratio is enhanced by using of fast Fourier transform of the analyte and signal integration [21,22]. FFTCCV can be considered as a new sensitive, accurate and fast method for determination of drugs and some pesticides. However, in order to obtain better sensitivity for a specific target, experimental parameters should be optimized. The optimum feed pH, feed flow rate, ATChCl concentration and sweeping-rate were found to be 7.4, 0.34 mL min^{-1}, 0.750 mM and 10 V s^{-1}, respectively. The long-term stability of this flow-through system was 80% of its initial response after 120 days. On the basis of the inhibition of OPs on the enzymatic activity of AChE, the conditions for OP detection were optimized using paraoxon as a model OP compound. The inhibition of paraoxon was proportional to its concentration range from 2.5×10^{-7} to 20 mg L^{-1} and was linear with −log [paraoxon] at the concentration range of 2.5×10^{-7} to 0.05 mg L^{-1}, with a detection limit of 1.7×10^{-7} mg L^{-1} (6.2×10^{-13} M). This study provides a new, modern, sensitive tool for the analysis of organophosphate pesticides. The results showed that the detection limit for paraoxon was 6.2×10^{-13} M, based on a 0.1 mL injection of 6.2×10^{-17} mol paraoxon. This detection limit is about 1000 times lower than that of the most sensitive method reported to date [23]. This system has good long-term stability, and the flow-through system with a fixed bed-reactor and the novel enzyme-immobilization method permitted high catalyst loading and low detachment, which could also be of interest in other sensors.

References

[1] P.S. Chen, S.D. Huang, Talanta 69 (2006) 669–675.
[2] W.N. Aldridge, Biochem. J. 46 (1950) 451–460.
[3] D. Du, J. Wang, J.N. Smith, C. Timchalk, Y. Lin, Anal. Chem. 81 (2009) 9314–9320.
[4] B.O. Luciana, S. dos, M.C.C. Infante, J.C. Masini, Anal. Bioanal. Chem. 396 (2010) 1897–1903.
[5] L. Gorton, E. Csöregi, E. Domínguez, J. Emnéus, G. Jönsson-Pettersson, G. Marko-Varga, B. Persson, Anal. Chim. Acta 250 (1991) 203–248.
[6] J. Wang, C.T. Chalk, Y. Lin, Environ. Sci. Technol. 42 (2008) 2688–2693.
[7] I. Shitanda, S. Takamatsu, K. Watanabe, M. Itagaki, Electrochim. Acta 54 (2009) 4933–4936.
[8] D.J. Bealea, N.A. Portera, F.A. Roddickb, Talanta 78 (2009) 342–347.
[9] W. Kaewthong, S. Sirisansaneeyakul, P. Prasertsan, A. Hkittkun, Process Biochem. 40 (2005) 1525–1530.
[10] P. Norouzi, M.R. Ganjali, A.A. Moosavi-movahedi, B. Larij, Talanta 73 (2007) 54–61.
[11] P. Norouzi, B. Larijani, M. Ezoddin, M.R. Ganjali, Mater. Sci. Eng. C 28 (2008) 87–93.
[12] P. Norouzi, P. Daneshgar, M.R. Ganjali, Mater. Sci. Eng. C 29 (2009) 1281–1287.

[13] B. Akbari-adergani, P. Norouzi, M.R. Ganjali, R. Dinarvand, Food Res. Int. 43 (2010) 1116–1122.
[14] F.M. Hawkridge, in: P.T. Kissinger, W.R. Heineman (Eds.), Laboratory Techniques in Electroanalytical Chemistry, 2nd ed., Marcel Dekker, New York, 1996.
[15] J.C. Myland, K.B. Oldham, J. Electroanal. Chem. 535 (2002) 27–35.
[16] B. Vivek, L. Kandimalla, J. Huangxian, Eur. J. Chem. 12 (2006) 1074–1080.
[17] K. Anitha, S. Venkata Mohanb, S. Jayarama Reddya, Biosens. Bioelectron. 20 (2004) 848–856.
[18] M.R. Ganjali, P. Norouzi, M. Ghorbani, A. Sepehri, Talanta 66 (2005) 1225–1233.
[19] P. Norouzi, M.R. Ganjali, T. Alizadeh, P. Daneshgar, Electroanalysis 18 (2006) 947–954.
[20] P. Norouzi, M.R. Ganjali, M. Ghorbani, A. Sepehri, Sens. Actuators B Chem. 110 (2005) 239–245.
[21] A.S. Baranski, P. Norouzi, L.J. Nelsson, Proc. Electrochem. Soc. 9 (1996) 41.
[22] E.O. Brigham, The Fast Fourier Transform and Its Applications, Prentice-Hall Inc., Englewood Cliffs, 1988.
[23] Y. Lin, L. Guodong, J. Wang, Anal. Chem. 78 (2006) 835–842.